Macromolecules

ARTICLE

pubs.acs.org/Macromolecules

Influence of Surfactants on Hydrophobically End-Capped Poly(ethylene oxide) Self-Assembled Aggregates Studied by SANS

Chantal Rufier,[*,†,⊥] André Collet,[†] Michel Viguier,[†] Julian Oberdisse,[*,‡,§] and Serge Mora[‡]

[†]Institut Charles Gerhardt UMR-CNRS 5253 and [‡]Laboratoire Charles Coulomb L2C, UMR-CNRS 5221, Université Montpellier 2, Pl. E. Bataillon, F-34095 Montpellier Cedex 05, France

[§]Laboratoire Leon Brillouin, CEA Saclay, F-91191 Gif Sur Yvette, France

Supporting Information

ABSTRACT: The rheological properties of associative polymers (APs) are modified by the presence of surfactants, but little is known about the influence of surfactants on the structure of self-associated aggregates in aqueous media. Using small-angle neutron scattering (SANS), the structure of self-assembled aggregates of a series in concentration of telechelic poly(ethylene oxide) ($M \approx 20\,000$ g mol^{-1}) end-capped by hydrocarbon or of fluorocarbon groups in the presence of a fixed amount of sodium dodecyl sulfate (SDS) or lithium perfluorooctyl sulfonate (LiFOS) is investigated. In all systems studied, surfactants and telechelic polymers form mixed aggregates. Their aggregation numbers are reduced and evolve with the concentration of each component. For example, with SDS at 8 mM, the mixed aggregates are composed of 1 AP and 15 SDS or 9 APs and 45 SDS molecules for 1 or 3 wt % of polymer, respectively. The addition of a surfactant enhances the number density of aggregates, which causes the increase of the gel viscosity.

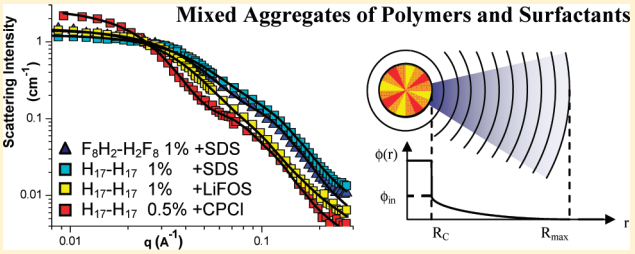

1. INTRODUCTION

The behavior of associative polymers (APs) in an aqueous phase can be significantly modified by the presence of a surfactant. The most common systems investigated are composed of a telechelic hydrophobically modified poly(ethylene oxide) (HMPEO) as the nonionic amphiphilic polymer and sodium dodecyl sulfate (SDS) as the anionic surfactant.[1−8] A small amount of surfactant is enough, in most cases, to prevent the aqueous phase segregation occurring with HMPEO end-capped by highly hydrophobic end groups. For instance, it was found that the ternary system SDS/HMPEO/water, involving perfluorinated end-capped PEO, is homogeneous with a molar ratio SDS/HMPEO equal to 0.3.[9] The role of the surfactant is not limited to the homogeneization of AP solutions in water; the surfactant also influences the AP rheological behavior in aqueous solution. The viscosity increases with addition of surfactant until a concentration close to the surfactant critical micelle concentration (cmc), but an excess of SDS totally disrupts the polymer transient network and induces a drastic decrease of viscosity.[6,10,11] Moreover, we have shown that the structure of HMPEO aggregates can be profoundly modified by the presence of SDS.[12]

In the dilute regime, characterized by a low viscosity of aqueous solutions, the self-assembled aggregates are noninteracting. Three critical transitions have been established as a function of SDS concentration. The first, at low surfactant concentration, corresponds to the uncooperative bonding (C_{ub}) between SDS and AP flower-like aggregates, leading to the formation of mixed aggregates. With increasing SDS concentration, the onset of cooperative binding is observed beyond the critical aggregation concentration (cac). This transition, driven by the surfactant, leads to the formation of micellar aggregates mainly constituted of SDS molecules wrapped by the PEO chain with a necklace-like conformation. The critical concentration C_m occurs at higher surfactant concentration and corresponds to the saturation of PEO chains by surfactant.

Small-angle neutron scattering (SANS) is a powerful technique to investigate the aggregate structure. By this method, the average size and the aggregation number of flower-like aggregates have been determined in the AP dilute regime. In the semidilute regime, above the threshold AP concentration C^*, corresponding to the sol−viscoelastic transition, the aggregate structure is governed by AP self-association. The aggregates are interconnected, leading to the formation of a transient network. SANS can provide information on the different types of interactions occurring between aggregates and the average interaggregate distance (D). A few SANS studies have previously investigated the binary HMPEO/water systems.[13−17] Binding interactions between SDS and HMPEO in the ternary system are even more complex. Depending on SDS and AP concentrations, uncooperative or cooperative binding can be the dominant process. Cooperative binding interactions between SDS micelles and PEO chain depend on polymer molecular weight.[18,19] The SDS/PEO aggregation complex resulting from polymer-induced

Received: May 19, 2011
Revised: August 8, 2011
Published: August 26, 2011

surfactant micellization involves SDS micelles with lower aggregation number than those observed in pure water.[20] The size, shape, stoichiometry, and internal organization of SDS/PEO aggregates in dilute aqueous solution were determined by Cabane and Duplessix using SANS.[21,22] The main conclusions drawn from this last study show that each aggregate contains a single PEO chain with SDS molecules clustered in spherical subunits (20 Å in radius) and adsorbed on the polymer backbone.

A few SANS studies have been performed on modified PEO in presence of surfactants. Appell et al. investigated the interactions between nonionic surfactant ($C_{12}EO_6$) and polymer ends capped by dodecyl groups.[23] Concentrations were chosen to keep the number of hydrophobic groups constant, and the molar ratio of polymer over surfactant was changed. This study showed formation of mixed aggregates, the size of which stays relatively constant, with about 100 hydrophobic groups. Recently, Ramos and Ligoure[24] and Lodge et al.[25] studied solutions of worm-like micelles of cationic surfactants mixed with telechelic polymers. Concentrations of each compound were chosen to preserve the structure of the worm-like micelles, such that the telechelic polymers link the micelles and increase the viscosity of the solution. However, we have not found in the literature any SANS study devoted to ternary systems anionic surfactant/HMPEO/water in dilute solution.

In a recent paper, we have investigated, by ^{13}C NMR and SANS, the interactions between hydrophobically end-capped PEO and SDS.[12] Using the SDS hydrocarbon tail as an internal probe, NMR data produced information on the local environment inside mixed aggregates, while the aggregation numbers and size of aggregates were determined by SANS experiments in the Guinier range. In the present paper, we investigate the structure of surfactant/HMPEO aggregates, obtained with different surfactants (anionic or cationic, fluorinated, or protonated) and various AP hydrophobic end groups (hydrocarbon or fluorocarbon). To improve the understanding of the influence of surfactant chemical structure on the aggregation process, this study involves hydrocarbon surfactants SDS, cetylpyridinium chloride (CPCl), and lithium perfluorooctyl sulfonate (LiFOS). Experimental data on structure and composition of aggregates are so far only available for SDS/PEG/H_2O[21,22] or HMPEO/H_2O[16] systems. This study was also focused on the conformation of PEO chains in the dilute and semidilute regime. Different models have been applied to fit scattering experimental curves.

In the present study, surfactant concentrations were kept at their cmc, and the HMPEO concentration was increased from the dilute regime to semidilute regime. The results will be presented for each regime separately because they have different structures. For both regimes, first data treatment will be shown by comparison with theoretical models, and then the influence of the surfactant and the polymer concentration will be treated. Finally, the relationship between the new results and the known rheological behavior of the ternary system will be discussed.

2. EXPERIMENTAL METHODS

2.1. Sample Preparation and Characterization. Symmetric telechelic HMPEO were synthesized by esterification of poly(ethylene glycol) (M_w = 20 000 g/mol) with carboxylic acids in presence of *N,N*-dicyclohexylcarbodiimide (DCC) and (dimethylamino)pyridine (DMAP) as described by Hartmann et al.[26] HMPEO obtained by this method were end-capped by hydrocarbon groups $C_{17}H_{35}$-(PEO)-$C_{17}H_{35}$ (denoted H_{17}-H_{17}) or semifluorinated ones C_8F_{17}-C_2H_4-PEO-C_2H_4-C_8F_{17} (F_8H_2-H_2F_8) and C_8F_{17}-$C_{10}H_{20}$-PEO-$C_{10}H_{20}$-C_8F_{17} (F_8H_{10}-$H_{10}F_8$).[9] Complete functionalization of PEO was controlled by titration of residual hydroxy groups by ^{19}F NMR according to a method described previously.[26] The persistence of the polymer chain length after the esterification was verified by size exclusion chromatography (SEC) using a set of two PLgel columns with pore sizes 10^3 and 10^4 Å and a Shimadzu differential refractometer. To prevent polar interactions between HMPEO and the gel phase, a solution of tetrabutylammonium bromide in tetrahydrofuran (10 mM) was used as eluent (flow rate 1 mL min^{-1}). HMPEO average molecular weights and polydispersity indices were determined from calibration against poly(ethylene oxide) standards. The poly(ethylene glycol) of molecular weight of 20 000 g/mol supplied by Merck was found to be 19 000 g/mol with a polydispersity index of 1.15.

Sodium dodecyl sulfate (Aldrich), cetylpyridinium chloride (Aldrich), and lithium perfluorooctyl sulfonate (kindly supplied by Atochem) were used as received without further purification.

Samples were prepared in pure D_2O, stirred until they were monophasic, and stored for 1 week in an opaque box at room temperature to let the system reach the equilibrium.

2.2. Small-Angle Neutron Scattering (SANS). SANS measurements were carried out at Laboratoire Léon Brillouin (Saclay, France). The data were collected on instrument PACE at two configurations, 7 and 8 Å, with respective sample-to-detector distances 1 and 4.5 m, covering a scattering vector (q) range of 0.06−2.8 nm^{-1}. Samples were prepared in pure D_2O, and 2 mm light path Hellma quartz cells were used. Empty cell scattering was subtracted, and the detector was calibrated with 1 mm H_2O scattering. All measurements were carried out at 25 °C. These data were converted to absolute intensity through a direct beam measurement, and the incoherent background was estimated with H_2O/D_2O mixtures. The modeling of SANS data is detailed in the Supporting Information. Data fitting was partially performed using SASfit ver. 0.90.1 software package developed by J. Kohlbrecher and I. Bressler, which is freely available on the Web (http://kur.web.psi.ch/sans1/SANSSoft/sasfit.html).

3. RESULTS

The concentrations of HMPEO solutions in D_2O, studied by SANS, ranged between 0.5 and 5 wt %. In the purely viscous dilute regime, and beyond the polymer cac = 10^{-4} wt %, HMPEO are self-associated in flower-like aggregates so HMPEO should be aggregated in the studied solutions. All neutron scattering experiments were performed in presence of surfactant concentrations equal to the cmc in pure water: C_{SDS} = 8 mM, C_{CPCl} = 1.2 mM, and C_{LiFOS} = 4 mM. In a previous paper,[12] we presented a ^{13}C NMR study of these systems. We showed that the surfactant cac in the ternary systems SDS/HMPEO/water, determined by ^{13}C NMR, was found to be lower than the SDS cmc and constant within the polymer concentration range studied (SDS cac = 4 mM).[12] In the dilute regime, beyond the polymer cac and below the critical concentration C^* of transient networks (cac < C_{pol} < C^* where cac = 10^{-4} wt % and C^* = 1 wt %), aggregates are organized in a cooperative binding with the necklace-like conformation of PEO chains, wrapped around micellar aggregates. In the viscoelastic semidilute regime ($C_{pol} > C^*$), the structure of mixed aggregates and bridging between aggregates leads to the formation of a transient network governed by the APs.

Figure 1 shows the variations of scattered intensity (I) versus scattering vector (q) for different concentrations of H_{17}-H_{17} AP with SDS at 8 mM. The curve shape changes between the dilute and the semidilute regime. At higher polymer concentrations, curves exhibit a peak at the wave vector position (q_{max}) which is

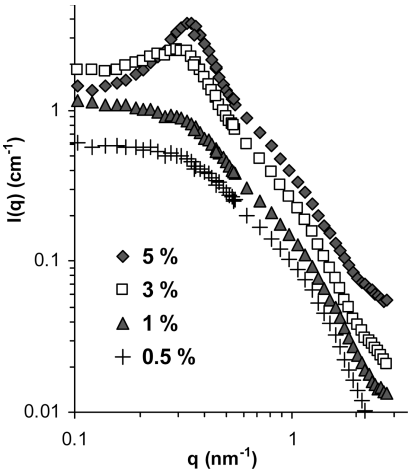

Figure 1. Scattering intensities from aqueous solutions of telechelic polymer H_{17}-H_{17} for C_{pol} = 0.5, 1, 3, and 5 wt %, with SDS (8 mM).

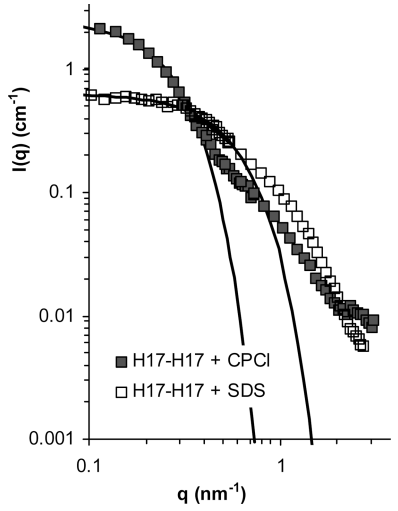

Figure 2. Neutron scattered intensities from dilute aqueous solutions of telechelic polymer H_{17}-H_{17} at C_{pol} = 0.5 wt % in the presence of SDS (8 mM) (□) or CPCl (1.2 mM) (■). The solid lines are the asymptotic behavior derived from the Guinier approximation.

related to the liquid-like ordering of aggregates and provides information on the most probable interaggregate distance D. The structure of aggregates and conformation of PEO chains, according to surfactant nature, will be investigated separately in the dilute and semidilute regime, detailed in sections 3.1 and 3.2, respectively. For each regime, first data treatment will be presented by comparison with theoretical models, and then the influence of the surfactant and the polymer concentration will be discussed.

3.1. Dilute Regime. *3.1.1. Comparison with Theoretical Models.* The fitting details are reported in the Supporting Information. The simplest method to study the scattering intensity in the dilute regime is to use the Guinier approximation, which can be expressed as

$$I(q) = I_0 \exp\left(\frac{-q^2 R_g^2}{3}\right) \quad (1a)$$

This approximation is relevant for small wave vector ($qR_g < 1$) and for form factor scattering only. It gives the radius of gyration

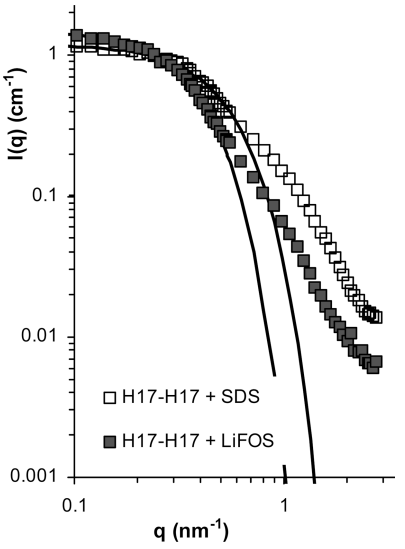

Figure 3. Scattered intensities for H_{17}-H_{17} in D_2O at 1 wt % in presence of SDS (8 mM) (□) or LiFOS (4 mM) (■). The solid lines are the asymptotic behavior derived from the Guinier approximation.

Table 1. Structural Parameters of Self-Assembled Aggregates Involving Surfactant and/or Associative Polymer H_{17}-H_{17} in Dilute Solution

surfactant	C_{pol} (wt %)	R_g (nm) ± 0.1	p_{AP}[a] (±10%)	p_S[a] (±10%)
CPCl	0	1.9		104
SDS	0	1.6		66
CPCl	0.5	6.6	5	26
SDS	0.5	3.0	0.7	23
SDS	1	3.3	1	15

[a] p_{AP} and p_S are respectively the average partial aggregation numbers of associative polymer and surfactant.

R_g of aggregate, and via the intensity I_0 at $q \to 0$, the dry particle volume V_0 can be determined with

$$I_0 = \Phi V_0 \rho^2 \quad (1b)$$

Φ is the volume fraction of the aggregate, and ρ is its scattering length density. The value of V_0 is directly related to the average molar mass of the aggregate and consequently to the aggregation numbers p_i by

$$V_0 = \sum_i V_i p_i \quad (1c)$$

where V_i is defined as the volume of molecule i. This holds if all aggregates are identical which means that the proportion of i in the aggregate is equal to its proportion in the entire solution. We will comment on the validity of this hypothesis later in the paper. Examples of fits are given in Figures 2 and 3. The radius of gyration R_g and the aggregation numbers p_i of all the dilute samples are reported in Tables 1 and 2.

For a detailed interpretation, the scattering intensities were compared with theoretical models. The most common expressions of model form factors were summarized by Pedersen.[27] Pedersen also developed a model based on a dense spherical core of hydrophobic segments surrounded by a shell of Gaussian polymer chains grafted to the surface.[28,29] The form factors based

Table 2. Surfactant and AP/Surfactant Self-Assembled Species in Aqueous Solution[a]

polymer	surfactant	R_g (nm) (±0.1)	p_{AP} (±10%)	p_S (±10%)
	LiFOS	1.2		25
	SDS	1.6		66
H_{17}-H_{17}	LiFOS	4.6	1.9	15
H_{17}-H_{17}	SDS	3.3	1.0	15
F_8H_2-H_2F_8	LiFOS	4.2	1.5	12
F_8H_2-H_2F_8	SDS	3.9	1.2	19

[a] The polymer concentration in ternary systems is 1 wt %.

on these models do not fit our experimental data correctly. As observed previously,[14] in the intermediate region ($0.5 < q < 2$ nm^{-1}), the scattering intensities from telechelic polymers present a bump that was ascribed to the small core of the aggregates. We could not fit this bump with the Pedersen model in a satisfactory way.

Other authors suggested that the aggregates of telechelic polymers can be assimilated with starlike polymers.[14,15,30] In the model proposed by Daoud and Cotton,[31] every polymer branch of the corona is constituted by a succession of blobs, the size of which increases from the center of the star to the outer corona. Moreover, Wijmans et al.[32] established that polymers grafted on small spheres have a volume fraction profile following the scaling law $\Phi \sim r^{-4/3}$ in good solvent.

The intensity of diluted particles composed of concentric shells can be described by the eq 2:

$$I(q) = I_0 \int_0^\infty 4\pi r^2 \frac{\sin qr}{qr} \rho(r)\, dr \qquad (2)$$

We will use this equation either for a density profile $\rho(r)$ of a given functional form of the shell (exponential profile in the shell, ExpShell model, cf. eqs S6−S8 in Supporting Information) or for a model with a free profile (MultiShell model). In the empirical model with the exponential profile in the shell (ExpShell model), the core radius was fixed by the aggregation numbers obtained by the Guinier approximation, considering all the hydrophobic groups to be in the dense core. This ExpShell model was found to provide accurate fits of our data in the low-q range. To achieve perfect fits, an additional, low-amplitude term had to be added based on the approach by Dozier[33] et al., who empirically added a monomer correlation term (cf. eq S9 in Supporting Information). This model has been successfully used in the literature for star polymers and polymer−nanoparticle hybrid aggregates.[34−36] In the dilute regime of HMPEO, the contribution of internal structure (Dozier monomer correlation term) is below 2% at low angles and becomes significant only at large angles. However, due to the addition of uncorrelated terms, the approach by Dozier et al. is not self-consistent. For comparison, we have also applied our MultiShell model recently developed for diblock copolymer systems[37] which is also based on eq 2 (see Supporting Information for fitting details). In this MultiShell model, the monomers are distributed over concentric spherical shells around the hydrophobic core as shown in Figure 4.

In the MultiShell model, the volume fraction profile was free. The monomers were distributed over typically 10−15 shells of 0.75 nm of thickness and then organized by Monte Carlo steps to optimize the agreement with the experimental curves $I(q)$, under the constraint of a smooth profile. The experimental and calculated scattering curves obtained with the different systems

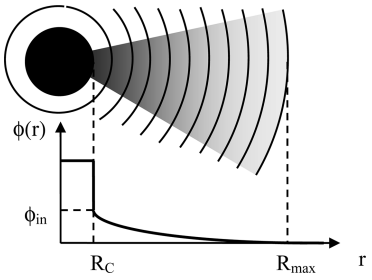

Figure 4. Schematic representation of associative polymer aggregate contrast as MultiShell model. The local volume fraction $\phi(r)$ profile, in dilute regime, as a function of the distance r from the aggregate core center.

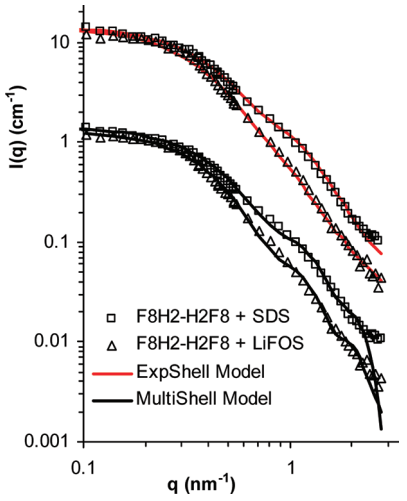

Figure 5. Scattered intensities for F_8H_2-H_2F_8 in D_2O at 1 wt % in presence of SDS (8 mM) (□) or LiFOS (4 mM) (△). Experimental data are fitted by the theoretical calculations according to the ExpShell model (red solid lines, on top) and to the MultiShell model (black solid lines, on bottom). For clarity, the experimental intensities are reported twice and are multiplied by 10 with the ExpShell model fit.

involving hydrocarbon and fluorinated end-capped PEO, in the presence of various types of surfactants, are compared in Figures 5 and 6. These figures show a comparable quality of the fits everywhere but in the highest q-range, where the finite shell size becomes visible, and the intensity is very low anyway. The volume fraction profile obtained by the MultiShell model for the H_{17}-H_{17} with each surfactant is shown in Figure 7. The main results of the two models (ExpShell model and MultiShell model) are the radius of the core R_c, the radius of the shell R_{max}, and the polymer volume fraction in the shell Φ. They are reported in Table 3.

The first result of this modeling is the aggregation numbers obtained from I_0 (cf. Tables 1 and 2) that we can compare to the aggregation number of associative polymers or surfactants alone in solution. According to previous studies on homologous polymers,[14,16,17] the telechelic polymer alone in solution forms micelles of 20−50 polymers such that the scattering intensity I_0 at low q should be between 8 and 21 cm^{-1} for a 0.5 wt % solution. With all the studied surfactants, the value of I_0 is between 0.6 and 2 cm^{-1} for the same polymer concentration (Figure 2). Given the small change in contrast and volume fraction, the strong decrease of I_0 clearly shows that there is no flower-like aggregate

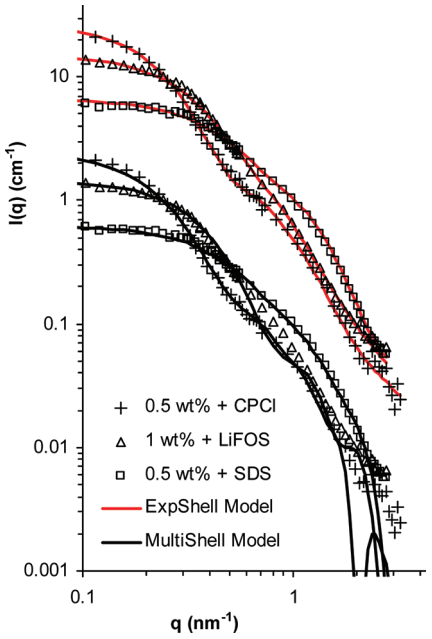

Figure 6. Comparison between experimental data and theoretical calculations for H_{17}-H_{17} in D_2O at 0.5 or 1 wt % in presence of various surfactants: SDS (8 mM) (□), LiFOS (4 mM) (△), CPCl (1.2 mM) (+). Experimental data are fitted by the theoretical calculations according to the ExpShell model (red solid lines, on top) and to the MultiShell model (black solid lines, on bottom). For clarity, the experimental intensities are reported twice and are multiplied by 10 with the ExpShell model fit.

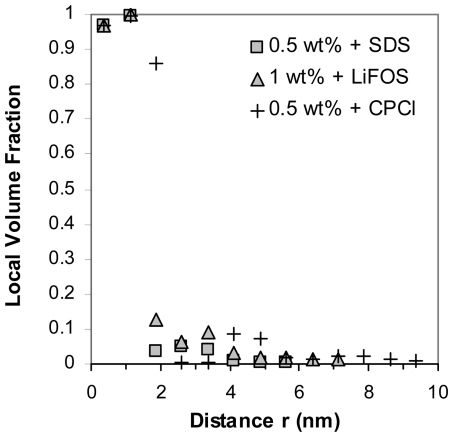

Figure 7. Local volume fraction profile in aggregates obtained with the MultiShell model for H_{17}−H_{17} in D_2O at 0.5 or 1 wt % in presence of various surfactants: SDS (8 mM) (□), LiFOS (4 mM) (△), CPCl (1.2 mM) (+).

with 20 polymers. Surfactants and APs form mixed aggregates with highly reduced aggregation numbers (cf. Tables 1 and 2).

The size of the core cannot be directly determined by the Guinier approximation. Nevertheless, considering all the hydrophobic groups to be in a dense core, we calculate a core radius R_c which was used in the ExpShell model. Theoretical R_c is between 1.2 and 1.7 nm according to the surfactant and the polymer concentration (cf. Table 3). With the MultiShell model, the volume fraction profile was not predetermined, and a profile with a dense core and very swollen polymer in external shells was spontaneously obtained. The core sizes obtained with the

Table 3. Structural Parameters[a] of Mixed Aggregates Obtained with the ExpShell Model and the MultiShell Model

			ExpShell model			MultiShell model		
polymer	C_{pol} (wt %)	surfactant	R_c (nm)	R_{max} (nm)	ϕ_{in}	R_c (nm)	R_{max} (nm)	ϕ_{av}
H_{17}-H_{17}	0.5	SDS	1.35	8.35	0.035	1.12	5.6	0.024
H_{17}-H_{17}	1	SDS	1.2	8.5	0.040	1.12	7.1	0.025
H_{17}-H_{17}	1	LiFOS	1.3	10.3	0.035	1.12	7.1	0.047
H_{17}-H_{17}	0.5	CPCl	1.7	13.7	0.08	1.9	10.8	0.023
F_8H_2-F_8H_2	1	SDS	1.3	9.1	0.05	1.12	7.1	0.022
F_8H_2-F_8H_2	1	LiFOS	1.3	9.3	0.032	1.12	7.1	0.027

[a] R_c is the core radius; R_{max} is the external limit of the shell; ϕ_{in} is the volume fraction of associative polymer on the inner side of the shell ($r = R_c$); Φ_{av} is the average volume fraction of polymer in the shells for $r > R_c$.

MultiShell model are very close to the theoretical ones deduced from the aggregation numbers (cf. Table 3), which confirms the core−shell conformation of the aggregates. A polydispersity of the core radius can be added in the ExpShell model. The best fits were obtained with a polydispersity of 30, 40, and 25% with SDS, LiFOS, and CPCl, respectively, independently of the AP. Note that polydispersity of aggregates supposing well-defined interfaces (as implicit in the ExpShell model) could in principle be extracted from the Multishell model using thinner shells but was not implemented.

In all studied systems, the hydrophobic dense core is surrounded by swollen PEO chains. In the ExpShell model, the polymer volume fraction decreases exponentially in the shell, and the density maximum, close to the core, is very low (0.035, 0.04, and 0.08 for H_{17}-H_{17} with SDS, LiFOS, and CPCl, respectively; cf. Table 3). With the MultiShell model the polymer volume fraction stays low and relatively constant (cf. Table 3 and Figure 4). The PEO swelling is comparable to the one determined for telechelic associating PEO in pure water.[14] Because of the strong interactions between SDS and the PEO chain of the associative polymers, one could have expected a higher polymer volume fraction in the vicinity of the aggregate core (Φ_{in}). This is not the case, presumably due to the low SDS aggregation number.

To calculate the aggregation numbers, it was assumed that local micellar and global solution proportions were identical. The following reasons make us believe that this is a good assumption: (a) The theoretical curves obtained with this homogeneity assumption are compatible with the experimental intensities. (b) The core radius R_c calculated from the partial aggregation numbers was independently confirmed by the MultiShell model in which the aggregate shape was not predetermined. (c) Assuming the opposite extreme, i.e., coexistence of pure surfactant and copolymer micelles would lead to a large overestimation of the intensities, due to the bigger masses. In conclusion, the mixed aggregates are likely to have the same composition than the entire solution.

3.1.2. Effect of the Surfactant. ***Role of the Counterion.*** It is well-known that anionic surfactants interact strongly with neutral polymers, whereas cationic ones show little affinity for these polymers.[38,39] However, it has been shown that significant interactions occur between water-soluble neutral polymers with a certain hydrophobic character (cellulose derivatives for example) and cationic surfactants (alkylammonium[40−43] and pyridiniums[42] salts). It is therefore relevant to study the interactions between a

cationic surfactant (CPCl) and an amphiphilic end-capped PEO with a well-defined architecture.

Figure 2 displays the variations of the scattered intensity $I(q)$ for H_{17}-H_{17} in the presence of SDS and CPCl. For the CPCl/H_{17}-H_{17}/D_2O and SDS/H_{17}-H_{17}/D_2O ternary systems, the asymptotic scattering functions at low wave vector q are well reproduced by a Guinier approximation. As noted above, the low I_0 values compared with I_0 of flower-like AP aggregates clearly proves the mixed aggregate formation with both surfactants. The radius of gyration (R_g) of aggregates can be estimated from the change in curvature of the scattering curve. This specific point is shifted toward higher q values in the presence of CPCl and even more with SDS, indicating that the overall dimensions of mixed aggregates are reduced (cf. Table 1). As explained earlier, the average composition and aggregation number (p) can be determined from the I_0 intensity (cf. eq 1), supposing identical composition of all aggregates (Table 1). The aggregation number of CPCl, which is drastically reduced in the presence of H_{17}-H_{17}, proves fairly strong interactions between HMPEO and CPCl. Moreover, the AP aggregation number (p_{AP}) is also reduced in presence of CPCl but remains higher than the one observed with SDS. It is widely assumed that cationic surfactants (alkylammonium salts) do not interact with PEO, the strength of the interactions decreasing with the augmentation of the counterion radius.[38,39] Therefore, the binding interactions observed between amphiphilic polymer H_{17}-H_{17} and CPCl are due to hydrophobic end groups involving a CPCl cooperative binding process with formation of mixed aggregates.

In the ternary system surfactant/HMPEO/water, the total aggregate size is driven by different factors such as molecular volumes, hydrophilic−hydrophobic ratio, concentrations, and interactions between molecules. The drastically reduced size of the mixed aggregate could be due to a change of core surface curvature imposed by the associative polymer. The very low volume fraction of the hydrophobic segment over the volume of the entire polymer (about 4%) can impose a relatively high curvature of the core surface, and so a small core volume and small aggregation numbers. With SDS, additional interactions between the surfactant anionic head and the PEO chain are present. The PEO chain can wrap around the SDS micelle and stabilizes them with even smaller aggregation numbers. Thus, global interaction between SDS and HMPEO is stronger than between CPCl and HMPEO.

In conclusion, even if these results underline the influence of surfactant counterion on the structure of the aggregates (size, composition), they show that the driving force in self-association process is the interaction between hydrophobic groups of surfactant and telechelic polymer.

Influence of Perfluorinated Surfactant. Despite the poor affinity between hydrocarbon and fluorocarbon chains, investigations by ^{13}C NMR on ternary systems involving SDS and semifluorinated telechelic PEO in aqueous solution reveal the formation of mixed agregates.[12] As shown in Figure 3, in the low wave vector range, scattered intensities I_0 are markedly reduced in presence of fluorinated surfactant at its cmc in pure water. Moreover, it is interesting to compare the scattering intensities obtained for H_{17}-H_{17}/SDS and H_{17}-H_{17}/LiFOS systems. In the low q range, experimental intensities are very close. Characteristics of dilute aggregates determined in the Guinier regime are reported in Table 2. As it was observed with SDS, the LiFOS aggregation number is reduced by the presence of HMPEO. Polymer and surfactant partial aggregation numbers are comparable in both surfactant systems. The nature of surfactant hydrophobic tail (hydrocarbon or fluorocarbon) does not significantly modify the structure of mixed aggregates. This is consistent with results reported recently that emphasize similarity of the aggregation mechanism of perfluorinated surfactant with that observed between SDS and PEO according to the necklace model.[44,45]

3.1.3. Effect of the Polymer. Influence of the Polymer Concentration. Throughout this study, surfactant concentrations were kept constant but SANS experiments were done with two dilute solutions of hydrogenated polymers H_{17}-H_{17}, in the presence of SDS. Table 1 presents the results with 0.5 and 1 wt % of polymer. While the polymer concentration is doubled and the SDS concentration is kept at 8 mM, the polymer aggregation number increases from 0.7 to 1, and the SDS aggregation number decreases from 23 to 15. It is interesting to notice that the multiplication by two of the polymer concentration does not multiply by two the polymer aggregation number nor divide by two the SDS aggregation number. With the polymer concentration, the aggregate weight increases (from about 20 to 24 kg/mol of aggregates) together with the number density of aggregates in the solution (from about 3.6×10^{-4} to 5×10^{-4} mol of aggregates per liter). Increasing the polymer concentration thus induces the formation of heavier and more numerous aggregates containing each less SDS.

Cross-Influence of Hydrophobic PEO End Group and Surfactant. In a recent paper,[12] we have shown by ^{13}C NMR the formation of mixed aggregates between SDS and fluorinated end-capped PEO with a more pronounced influence of highly fluorinated C_8F_{17}-$(CH_2)_2$ end groups on the local environment of hydrocarbon SDS tail. Scattered intensities, reported in Figure 5 for F_8H_2-H_2F_8/SDS and F_8H_2-H_2F_8/LiFOS systems, are very close. Results obtained using the Guinier approximation (cf. Table 2) reveal that mass and volume of mixed aggregates are equivalent regardless of the nature of surfactant, hydrogenated or fluorinated. Moreover, structure and composition of mixed aggregates (R_g, partial aggregation numbers) are comparable in both hydrocarbon (H_{17}-H_{17}/surfactant) and fluorinated (F_8H_2-H_2F_8/surfactant) systems. The nature of the hydrophobic groups of surfactant and telechelic PEO is not the decisive parameter for the structure of self-assembled mixed aggregates.

3.2. Semidilute Regime. *3.2.1. Form and Structure Factors of Aggregates.* The scattering curves in the semidilute regime, above the sol/viscoelastic transition ($C_{pol} > C^* = 1$ wt %), exhibit a peak that reveals the organization of mixed aggregates for both SDS/AP and LiFOS/AP systems (cf. Figure 1). If we consider a simple cubic organization, the average distance D between the aggregate centers can be estimated from the peak position (q_{max}):

$$D = \frac{2\pi}{q_{max}} \tag{3}$$

Other locally liquid-like arrangement would yield comparable results. Assuming a uniform distribution of constitutive elements between aggregates with homogeneous composition, the aggregation number is given by $p = \Sigma_i p_i = \Sigma_i c_i N_a (V/N)$ where c_i is the molar concentration of species i and N is the number of aggregates in the volume V. The obtained parameters D and p_i are reported in Table 4.

The aggregation numbers p_i are used to calculate the radius R_c of the hydrophobic core considering all the hydrophobic groups to be in a dense core. The obtained values of R_c and N are used in the core−shell form factor model with an exponential decrease of profile in the shell with the Dozier term (ExpShell model, cf. eqs S6−S9 in Supporting Information) as used for dilute solutions.

Table 4. Characteristics of Aggregates for HMPEO at 3 wt % in the Presence of SDS (8 mM) or LiFOS (4 mM)[a]

surfactant	polymer	V_{HEG} (nm^3)	D (nm)	p_{AP} ± 10%	p_S ± 10%	R_c (nm) ± 0.1
SDS	H_{17}-H_{17}	0.532	21.0	8.5	45	1.87
	F_8H_2-H_2F_8	0.522	21.5	9	47	1.86
	F_8H_{10}-$H_{10}F_8$	0.765	26.0	16	85	2.42
LiFOS	H_{17}-H_{17}	0.532	25.0	14.5	39	2.02
	F_8H_2-H_2F_8	0.522	24.0	13.5	36	1.96
	F_8H_{10}-$H_{10}F_8$	0.765	28.0	19.5	51	2.35

[a] V_{HEG} is the volume of hydrophobic end group, and R_c is the radius of the dense hydrophobic spherical core.

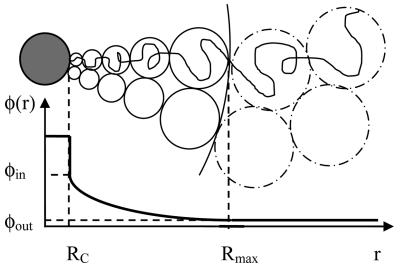

Figure 8. Schematic representation of star-like associative polymer aggregates and the local volume fraction profile in semidilute regime.

From the calculations, it appears that only 70% of the PEO has to be considered into the shell to obtain an intensity I_0, in agreement with the experimental points. Above the threshold concentration C^* = 1 wt %, in the semidilute regime, telechelic associative polymers develop a fully connected network of aggregates.[9] This transient network—which induces an increase of solution viscosity—is well described by the star-like polymer model proposed by Daoud and Cotton.[31] According to this model, the mixed aggregate structure in semidilute solution can be represented as in Figure 8.

For distances from the aggregate center larger than R_{max}, the overlapped polymer branches look like a "sea of blobs", the constant size of which is controlled by concentration. This "sea of blobs" is expressed by a higher contribution of the monomer—monomer correlation function in the form factor (Dozier term). Moreover, in semidilute solutions (3 and 5 wt %) a structure factor $S(q)$ that accounts for the interactions between aggregates must be incorporated in the calculation of $I(q)$. The rescaled mean spherical approximation (RMSA)[46,47] was introduced to take into account the presence of charged aggregates due to the ionic surfactant involved in the core of mixed aggregates. The best fits are obtained for an aggregate charge of 15, which is in agreement with the previous results of Bergstrom and Pedersen,[48] who found that about one-third of the SDS molecules are dissociated without added salt. The optimized parameters for SDS/H_{17}-H_{17}/D_2O system used to fit the experimental data by a combination of the RMSA structure factor and the ExpShell form factor (cf. Figure 9) are reported in Table S3 of the Supporting Information.

3.2.2. Cross-Influence of Hydrophobic End Group and Surfactant on the Aggregate Structure. Values of the distance between the centers of aggregate (D), ranging between 20 and 28 nm, are fairly dependent on the hydrophobic end group and surfactant (cf. Table 4). For the same surfactant, in this case SDS, but the trend holds generally, the volume of the hydrophobic end groups (V_{HEG}) influences D values more than the chemical structure of telechelic end-caps. Hydrocarbon $C_{17}H_{35}$- and semifluorinated $C_8F_{17}C_2H_4$- end groups with equivalent volumes lead to comparable D values and sizes of the aggregate core R_c. The higher V_{HEG} of semifluorinated end-caps C_8F_{17}-$(CH_2)_{10}$- influences both the size and the structure of the aggregates: the higher the V_{HEG}, the larger the aggregate core R_c.

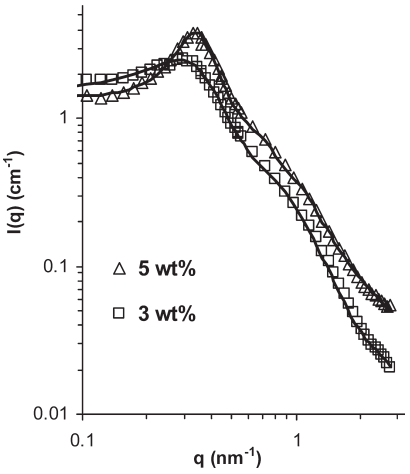

Figure 9. Experimental and calculated (solid lines) scattering intensities from semidilute aqueous solutions of telechelic polymer H_{17}-H_{17} in the presence of SDS (8 mM) at C_{pol} = 3 and 5 wt %.

The same evolution as a function of the end-caps is observed in the presence of the fluorinated surfactant (LiFOS). Nevertheless, the distances D and the size of aggregate core are shifted to higher values than with SDS. The influence of LiFOS can be correlated with a greater volume of LiFOS molecules 0.480 nm^3 vs 0.410 nm^3 with SDS and a larger AP aggregation number.

3.2.3. Effect of the Polymer Concentration. SANS experiments were done with two semidilute solutions (3 and 5 wt %) of hydrogenated polymers H_{17}-H_{17} in the presence of SDS as shown in Figure 9. The structural parameters obtained from the analysis of the experimental scattering curves (peak position) and theoretical fits (cf. Tables 4 and S3) clearly show important modifications of the aggregate structure in the semidilute regime compared with the dilute regime. The main conclusion is the growth of the aggregates above C^*, with an increase of the aggregation numbers (p_{AP} and p_S). As a consequence, the aggregate core size (R_c) and the thickness of the shell ($\Delta R = R_{max} - R_c$) are also increased (R_c = 1.9 or 1.75 nm and R_{max} = 10.9 or 9.75 nm, for 3 or 5 wt % of polymer, respectively).

One notes also a higher polymer volume fraction (ϕ_{in}) in the vicinity of the aggregation core (ϕ_{in} = 0.085 and 0.11 with 3 and 5 wt % of polymer, respectively).

At constant SDS concentration (8 mM), when the polymer concentration increases from 3 to 5 wt %, the polymer aggregation number increases from 8.5 to 9.5, and the SDS aggregation number decreases from 45 to 30. Even if they are still smaller, these mixed aggregates look more like a flower-like micelle than the mixed aggregates in dilute regime.

Furthermore, like in dilute regime, the multiplication by 1.7 of the polymer concentration does not multiply by 1.7 the polymer aggregation number nor divides by 1.7 the SDS aggregation number. Aggregates evolve with the concentration. The dynamic

system reorganizes itself and molecules are distributed again into a higher number of aggregates.

4. DISCUSSION

The original purpose in studying the surfactant−HMPEO interactions was to determine the role of surfactant on the self-organization processes of amphiphilic polymers and to understand the surfactant effect on rheological behavior of AP aqueous solutions previously reported.[6,9−11] The main observations on rheological behavior are reminded here: (a) the decrease of the critical concentration C^* with surfactant, (b) the almost perfect Maxwell behavior of gels, (c) the increase of viscosity η with a small quantity of surfactant by an increase of both the relaxation time τ and the elastic modulus G_0 ($\eta = G_0\tau$ for Maxwell fluids), (d) the drastic decrease of the viscosity at high surfactant concentrations, (e) in the same conditions, a higher relaxation time with a bigger hydrophobic group, and (f) in mixtures of hydrogenated and fluorinated species, the higher relaxation time if the AP and the surfactant have the same nature.

With ternary systems surfactant/associative polymer/water, different types of interactions (attractive or repulsive) occur: (i) Repulsive interactions between polymer chains swollen by water; in dilute aqueous regime these forces are relatively weak. (ii) Attractive interactions between surfactant molecules leading to the formation of micelles. (iii) Attractive interactions between anionic surfactants and PEO chains are strong enough depending on the surfactant; these forces stabilize the surfactant micelles with a reduced aggregation number. (iv) Attractive interactions between hydrophobic end groups of AP and surfactant hydrophobic tail; specific forces occurring in presence of HMPEO.

Structure and composition of aggregates are determined by the balance between the different forces operating as a function of component concentrations. It is known that the viscosity of AP aqueous solutions is modified by the presence of anionic surfactant, and the maximum of viscosity is obtained for a surfactant concentration close to the cmc in pure water.[11,49−51] The general assumption was that surfactant forms mixed aggregates with hydrophobic polymer end-caps, increasing the density of interaggregate connections. The results reported in this paper, obtained from SANS experiments, yield more precise information. The formation of mixed aggregates is now established as well as the composition of the aggregates. In all studied systems, the attractive interaction (iv) between hydrophobic groups is strong enough to lead to mixed aggregates. This specific interaction (iv) is the main leader to aggregation. More over, the AP aggregation number (p_{AP}) is lower in the presence of surfactant than without surfactant (p_{AP} values are ranging between 20 and 50 according to the chemical structure of hydrophobic group,[14,16,17,52] against 8 to 20 with C_{AP} = 3 wt % in the presence of anionic surfactants). The decrease of aggregation numbers implies a multiplication of aggregates and a decrease of the interaggregate distance (distance between surfaces of hydrophobic cores). For example, at 3 wt % pure H_{17}-H_{17} AP would form micelles of about 30 polymers which leads to an interaggregate distance of 28 nm and in the presence of SDS at 8 mM the distance is reduced to 17 nm, while the radius of gyration of the PEO chain is about 6 nm. Note that theoretical calculations[53] have shown that the onset of bridging takes place at approximately $3R_g$. So the increase in viscosity observed with surfactant can be attributed to the augmentation of the density of cross-linking sites, enhancing the density of elastically active bridging chains. This result is consistent with the increased values of the elastic modulus (G_0) in the presence of surfactant up to a certain concentration. The relaxation time (τ) is also enhanced by the presence of surfactant and contributes to the augmentation of viscosity η, as $\eta = G_0\tau$ in Maxwell fluids. The dominating process involved in the relaxation time was ascribed to the disengagement of the AP hydrophobic end group from the aggregate, τ corresponding to the lifetime of the aggregate junction.[54] The surfactant in the hydrophobic core should not influence the stability of the AP end-caps in the core; especially with nonionic or cationic surfactants, but shorter interaggregate distance increases the number of linking polymers as shown by the higher G_0 value. The probability to have more than one polymer liking two aggregates is higher,[53] leading to multiple bonds, and it was shown that the gel relaxation time τ increases with the connectivity of the network.[55,56] Thus, the reduction of aggregation numbers can explain the higher relaxation time via the multiple bonds.

In a previous rheological study,[11] we obtained unusual high τ values (τ > 100 s) with fluorinated APs with SDS compared to the τ values (τ = 14 s) for the same polymer alone in solution. This impressive increase has been correlated with the higher energy barrier associated with the disengagement of greatly hydrophobic fluorinated end groups. The higher τ values obtained in presence of surfactant cannot be ascribed to specific hydrophobic interactions (iv) inside the core of mixed aggregates. The thermodynamic compatibility between the polymer hydrophobic end groups and the surfactant tail influences the relaxation time; τ values are increased when hydrophobic groups have the same nature, which is not the case here, which implies other phenomena are probably operating. In the model proposed for the structure of mixed aggregates, PEO interacts with surfactant involved in the hydrophobic core of the aggregate. The specific interactions (iii) between anionic head of surfactant and PEO chain probably contribute to increase the energy needed for the hydrophobic end group disengagement.

In conclusion, these SANS results prove the evolution of the network morphology which was only assumption until now and give a different perspective to the role of surfactant in rheological behavior of transient network, with its specific interactions with APs. Yet another observed phenomenon is the network breakup when the surfactant is in excess. This breakup leads to a steep decrease of viscosity probably associated with a change of aggregate structure. SANS experiments could be a fruitful method to investigate this domain.

5. CONCLUSIONS

SANS studies of ternary systems involving telechelic polymer and surfactant bring new information on the structure of self-assembled entities. The formation of mixed aggregates with hydrophobic segments (surfactant tail and polymer end-caps) gathered in a dense core surrounded by a corona of PEO chains is now well established. The strong interactions between surfactant and PEO chains stabilize the self-assembled species, with lower aggregation numbers when compared with the homologous binary systems. Furthermore, the aggregate composition evolves with surfactant and AP concentrations, unlike the behavior of flower-like APs. These results prove general assumptions about these ternary systems, such as the formation of mixed aggregates, and the increase of the aggregate number. This explains the increase of the viscosity of these transient networks in presence of surfactant. In future, SANS could be used to study the effect of surfactant on the

rheological behavior of the gel, varying the surfactant concentration in different polymer solution. Especially the decrease of the viscosity with the excess of surfactant could be studied.

■ ASSOCIATED CONTENT

Supporting Information. Fitting details and parameters such as scattering length densities, form factor equations, obtained radius, and local volume fraction. This material is available free of charge via the Internet at http://pubs.acs.org.

■ AUTHOR INFORMATION

Corresponding Author

*E-mail chantal.rufier@insa-lyon.fr, Tel 33-472 43 63 35, Fax 33-472 43 85 27 (C.R.). E-mail julian.oberdisse@univ-montp2.fr, Tel 33-467 14 35 23, Fax 33-467 14 46 37 (J.O.).

Present Addresses

⊥Université de Lyon, INSA-Lyon, Ingénierie des Matériaux Polymères UMR5223, avenue Albert Einstein, F-69621 Villeurbanne Cedex, France.

■ REFERENCES

(1) Hu, Y. Z.; Zhao, C. L.; Winnik, M. A.; Sundararajan, P. R. *Langmuir* **1990**, *6*, 880–883.
(2) Binana-Limbele, W.; Clouet, F.; François, J. *Colloid Polym. Sci.* **1993**, *271*, 748–758.
(3) Annable, T.; Buscall, R.; Ettelaie, R.; Shepherd, P.; Whittlestone, D. *Langmuir* **1994**, *10*, 1060–1070.
(4) Abrahmsen-Alami, S.; Stilbs, P. *J. Phys. Chem.* **1994**, *98*, 6359–6367.
(5) Persson, K.; Wang, G.; Olofsson, G. *J. Chem. Soc., Faraday Trans.* **1994**, *90*, 3555–3562.
(6) Zhang, K.; Xu, B.; Winnik, M. A.; Macdonald, P. M. *J. Phys. Chem.* **1996**, *100*, 9834–9841.
(7) Dai, S.; Tam, K. C.; Jenkins, R. D. *Macromolecules* **2001**, *34*, 4673–4675.
(8) Dai, S.; Tam, K. C.; Wyn-Jones, E.; Jenkins, R. D. *J. Phys. Chem. B* **2004**, *108*, 4979–4988.
(9) Rufier, C.; Collet, A.; Viguier, M.; Oberdisse, J.; Mora, S. *Macromolecules* **2008**, *41*, 5854–5862.
(10) Amis, E. J.; Hu, N.; Seery, T. A. P.; Hogen-Esch, T. E.; Yassini, M.; Hwang, F. In *Hydrophilic Polymers*; Glass, J. E., Ed.; American Chemical Society: Washington, DC, 1996; Vol. 248, pp 279−302.
(11) Calvet, D.; Collet, A.; Viguier, M.; Berret, J.-F.; Séréro, Y. *Macromolecules* **2003**, *36*, 449–457.
(12) Rufier, C.; Collet, A.; Viguier, M.; Oberdisse, J.; Mora, S. *Macromolecules* **2009**, *42*, 5226–5235.
(13) François, J.; Maitre, S.; Rawiso, M.; Sarazin, D.; Beinert, G.; Isel, F. *Colloids Surf., A* **1996**, *112*, 251–265.
(14) Séréro, Y.; Aznar, R.; Porte, G.; Berret, J.-F.; Calvet, D.; Collet, A.; Viguier, M. *Phys. Rev. Lett.* **1998**, *81*, 5584 LP–5587.
(15) Beaudoin, E.; Borisov, O.; Lapp, A.; François, J. *Macromol. Symp.* **2002**, *191*, 89–97.
(16) Beaudoin, E.; Borisov, O.; Lapp, A.; Billon, L.; Hiorns, R. C.; François, J. *Macromolecules* **2002**, *35*, 7436–7447.
(17) Tae, G. Y.; Kornfield, J. A.; Hubbell, J. A.; Lal, J. S. *Macromolecules* **2002**, *35*, 4448–4457.
(18) Dai, S.; Tam, K. C. *J. Phys. Chem. B* **2001**, *105*, 10759–10763.
(19) Meszaros, R.; Varga, I.; Gilanyi, T. *J. Phys. Chem. B* **2005**, *109*, 13538–13544.
(20) Zana, R.; Lianos, P.; Lang, J. *J. Phys. Chem.* **1985**, *89*, 41–44.
(21) Cabane, B.; Duplessix, R. *J. Phys. (Paris)* **1982**, *43*, 1529–1542.
(22) Cabane, B.; Duplessix, R. *J. Phys. (Paris)* **1987**, *48*, 651–662.
(23) Appell, J.; Porte, G.; Rawiso, M. *Langmuir* **1998**, *14*, 4409–4414.
(24) Ramos, L.; Ligoure, C. *Macromolecules* **2007**, *40*, 1248–1251.
(25) Lodge, T. P.; Taribagil, R.; Yoshida, T.; Hillmyer, M. A. *Macromolecules* **2007**, *40*, 4728–4731.
(26) Hartmann, P.; Collet, A.; Viguier, M. *J. Fluorine Chem.* **1999**, *95*, 145–151.
(27) Pedersen, J. S. *Adv. Colloid Interface Sci.* **1997**, *70*, 171–210.
(28) Pedersen, J. S.; Gerstenberg, M. C. *Macromolecules* **1996**, *29*, 1363–1365.
(29) Pedersen, J. S. *J. Chem. Phys.* **2001**, *114*, 2839–2846.
(30) Semenov, A. N.; Joanny, J.-F.; Khokhlov, A. R. *Macromolecules* **1995**, *28*, 1066–1075.
(31) Daoud, M.; Cotton, J. P. *J. Phys. (Paris)* **1982**, *43*, 531–538.
(32) Wijmans, C. M.; Zhulina, E. B. *Macromolecules* **1993**, *26*, 7214–7224.
(33) Dozier, W. D.; Huang, J. S.; Fetters, L. J. *Macromolecules* **1991**, *24*, 2810–2814.
(34) Willner, L.; Jucknischke, O.; Richter, D.; Roovers, J.; Zhou, L.-L.; Toporowski, P. M.; Fetters, L. J.; Huang, J. S.; Lin, M. Y.; Hadjichristidis, N. *Macromolecules* **1994**, *27*, 3821–3829.
(35) Jin, S.; Higashihara, T.; Jin, K. S.; Yoon, J.; Rho, Y.; Ahn, B.; Kim, J.; Hirao, A.; Ree, M. *J. Phys. Chem. B* **2010**, *114*, 6247–6257.
(36) Berret, J.-F.; Yokota, K.; Morvan, M.; Schweins, R. *J. Phys. Chem. B* **2006**, *110*, 19140–19146.
(37) Ribaut, T.; Oberdisse, J.; Annighofer, B.; Stoychev, I.; Fournel, B.; Sarrade, S.; Lacroix-Desmazes, P. *Soft Matter* **2009**, *5*, 4962–4970.
(38) Wang, Y.; Han, B.; Yan, H.; Cooke, D. J.; Lu, J.; Thomas, R. K. *Langmuir* **1998**, *14*, 6054–6058.
(39) Benrraou, M.; Bales, B.; Zana, R. *J. Colloid Interface Sci.* **2003**, *267*, 519–523.
(40) Zana, R.; Binana-Limbele, W.; Kamenka, N.; Lindman, B. *J. Phys. Chem.* **1992**, *96*, 5461–5465.
(41) Bloor, D. M.; Mwakibete, H. K. O.; Wyn-Jones, E. *J. Colloid Interface Sci.* **1996**, *178*, 334–338.
(42) Carlsson, A.; Lindman, B.; Watanabe, T.; Shirahama, K. *Langmuir* **1989**, *5*, 1250–1252.
(43) Ghoreishi, S. M.; Fox, G. A.; Bloor, D. M.; Holzwarth, J. F.; Wyn-Jones, E. *Langmuir* **1999**, *15*, 5474–5479.
(44) Gianni, P.; Barghini, A.; Bernazzani, L.; Mollica, V. *Langmuir* **2006**, *22*, 8001–8009.
(45) Gianni, P.; Barghini, A.; Bernazzani, L.; Mollica, V.; Pizzolla, P. *J. Phys. Chem. B* **2006**, *110*, 9112–9121.
(46) Hayter, J. B.; Penfold, J. *Mol. Phys.* **1981**, *42*, 109–118.
(47) Hansen, J.-P.; Hayter, J. B. *Mol. Phys.* **1982**, *46*, 651–656.
(48) Bergstrom, M.; Skov Pedersen, J. *Phys. Chem. Chem. Phys.* **1999**, *1*, 4437–4446.
(49) Alami, E.; Almgren, M.; Brown, W. *Macromolecules* **1996**, *29*, 5026–5035.
(50) Kaczmarski, J. P.; Glass, J. E. *Macromolecules* **1993**, *26*, 5149–5156.
(51) Kim, D.-H.; Kim, J.-W.; Oh, S.-G.; Kim, J.; Han, S.-H.; Chung, D. J.; Suh, K.-D. *Polymer* **2007**, *48*, 3817–3821.
(52) Séréro, Y. PhD Thesis, University Montpellier 2, 1999.
(53) Testard, V.; Oberdisse, J.; Ligoure, C. *Macromolecules* **2008**, *41*, 7219–7226.
(54) Annable, T.; Buscall, R.; Ettelaie, R.; Whittlestone, D. *J. Rheol.* **1993**, *37*, 695–726.
(55) Michel, E.; Filali, M.; Aznar, R.; Porte, G.; Appell, J. *Langmuir* **2000**, *16*, 8702–8711.
(56) Puech, N.; Mora, S.; Testard, V.; Porte, G.; Ligoure, C.; Grillo, I.; Phou, T.; Oberdisse, J. *Eur. Phys. J. E* **2008**, *26*, 13–24.